Automatic Optical Inspection System of 3D Surface Profile of Unsymmetrical Microstructure Using Optical Interferometric Microscope

Shih-Wei Yang[1], Chern-Sheng Lin[2], Mau-Shiun Yeh[3]

1. Department of Electrical Engineering, Feng Chia University. Taichung, Taiwan.
2. Department of Automatic Control Engineering, Feng Chia University. Taichung, Taiwan.
3.Chung-Shan Institute of Science & Technology, Lung-Tan, Tao-Yuan, Taiwan.
E-mail: m9901655@mail.fcu.edu.tw

Abstract - In this paper, an automatic optical inspection system for the 3D surface profile of an unsymmetrical microstructure using a Fizeau interferometer, is proposed. This non-contact optical inspection system is suitable for measuring the lens sag and 3D surface profile of unsymmetric microlenses. The distribution of the interferometric fringes of unsymmetric microlenses is partly dense and partly rare, and is completely different from the equally dense distribution of symmetrical microlenses. Thus, a novel algorithm is proposed to overcome the above mentioned problem in this paper, namely, individually determining the darkest points of the dark fringes and the brightest points of the bright fringes, and fitting these determined points as close curves through the Bezier curve theory. As the contour lines of an unsymmetrical microstructure are obtained, the 3D surface profile of the unsymmetrical microstructure can be plotted correspondingly.

Keywords - 3D surface profile, unsymmetrical microstructure, Fizeau interferometer, Bezier curve.

I. INTRODUCTION

As present technology continuously pursues miniaturization, such as mobile phones, digital cameras, webcam lens of the notebook PC, etc., lenses must be miniaturized with the reduced volume of the main body. Therefore, a micro-lens with a radius of 10 μm to 2 mm is extensively used. The wafer-based process technology considers the accuracy degree of the lens profile surface[1-2], and determines the accurate location on the micro-lens array. Manual inspection may lead to different inspection results as the human eye would feel tired and make misjudgements after long hours of work. Therefore, this study designed an automatic inspection system that automatically obtains interference images of a micro-lens, according to the principle of the Fizeau interferometer [3-4], where noise is filtered through image processing to make the image clearer. The lens sag of a micro-lens was determined using an novel algorithm, and the micro-lens surface profile contour lines were built by computer graphics technology [5-6], which is able to restore the surface 3D pattern of a micro-lens.

Akihiro Yamamoto, and Yamaguchi used wavelength scanning Fizeau interferometry to measure the body surface profile and the surface profile height of aluminum coated glass surface. The surface profile of the object is measured by changing the interference signal phase [7]. Charriere et al. used digital holographic microscopy to describe the characteristics of a micro-lens [8], which allowed objects to be measured in a wide range of shapes as the vibration did not require isolation. However, the measurement structure for the surface shape of a micro-lens was incompatible with the measurement structure of the light characteristics of a micro-lens, and had to be measured by two instruments.

Therefore, this study proposed an innovative algorithm: to determine the darkest and brightest points of each dark fringe and bright fringe, and then use the Bezier curve to fit the determined points into a closed curve. These closed curves can be regarded as surface profile contour lines, which serve as the base for rebuilding the surface 3D pattern of the micro-lens.

II. METHODS FOR UNSYMMETRICAL MICROSTRUCTURE MEASUREMENT SYSTEMS

The interference fringes of micro-lens were obtained using the Fizeau interferometer principle of microscopic interferometry. The annular interference fringes contain dark fringe and bright fringe information are as shown in Fig. 1. In order to ensure that the fringes found in the image are extremely dark fringes and extremely bright fringes, the interference fringes of the unsymmetrical micro-lens are analysed according to the following procedures.

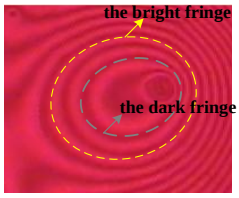

Fig. 1 Interference fringe image of unsymmetrical micro-lens

Fig. 2 Result of central point

A. Calculating Central Position of Micro-lens

Binarizing the original image (Figure 1), and then determining the central coordinates $C(X_c, Y_c)$ of the micro-lens using the region filling centroid method, as shown in the following equations and Figure 2.

$$X_c = \sum x / n. \quad (1)$$

$$Y_c = \sum y / n. \quad (2)$$

where $\sum x$ and $\sum y$ are the summation of x-coordinates and the summation of y-coordinates, n is the total pixels in this region.

B. Dividing Bright and Dark Fringes and Edge Point Searching

As the annular interference fringes are separated interference fringes, they are mutually exclusive and the division can be completed according to the concepts of "eight-neighbors" and "connectivity". As shown in Figure 3 (a)~(e), the dark fringes of each micro-lens can be divided into 5 tags (5 annular interference fringes); similarly, the bright fringe can be divided into 4 tags.

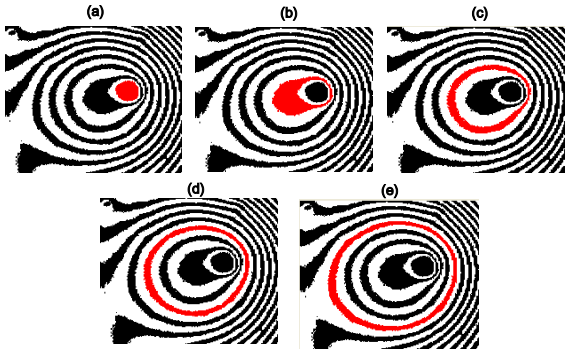

Fig. 3 Dark fringe division result (a) Loop 1 (b) Loop 2 (c) Loop 3 (d) Loop 4 (e) Loop 5

If the variation in brightness of two adjacent pixels is from dark to bright, and the gradient is 255, then the dark point must be the edge point of interference fringe. The complete interference fringe edge contour can be obtained by repeating this procedure. For example, the searched result for the edge point of the dark fringe is shown in Figure 4.

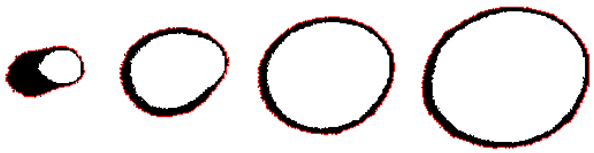

Fig. 4 Result of edge point of each dark fringe

C. Constructing The Radial Lines

The dark fringe is also taken as an example, where E_1, $E_2 \dots E_n$ represent the edge points of every dark fringe, and their coordinate points are (x_{e_1}, y_{e_1}), $(x_{e_2}, y_{e_2}) \dots (x_{e_n}, y_{e_n})$. Each edge point is connected to the central coordinate point C, and these connections are called radial lines. As shown in Figure 5, $\overline{CE_1}$, $\overline{CE_2}$, $\overline{CE_3} \dots \overline{CE_n}$ line segments represent the radial lines of connection between the edge points and center point.

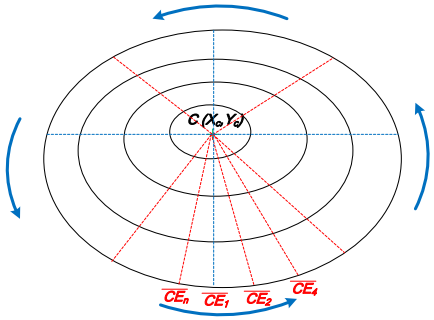

Fig. 5 Schematic diagram of radial lines of outermost dark fringe

Since the radial lines pass through every dark fringe, the extremely dark points of the radial lines in each interference fringe can be determined. Figure 6 shows the schematic diagram of the radial lines passing through the outermost dark fringe, where radial line No. n has k pixels R_{n1}~R_{nk}, herein $g(R_{11})$, $g(R_{12}) \cdots g(R_{1k})$ represent the gray scale values of k pixels passing through radial line $\overline{CE_1}$. Brightness is analyzed according to the gray scale values of k pixels in order to determine the coordinate point with the minimum brightness value, i.e. the extremely dark point of this radial line. Each dark fringe is calculated in the same way using a circular method to determine the extremely dark point on each dark fringe. In a similar manner, the coordinate point with the maximum brightness value among k pixels is determined to identify the extremely bright point of each bright fringe.

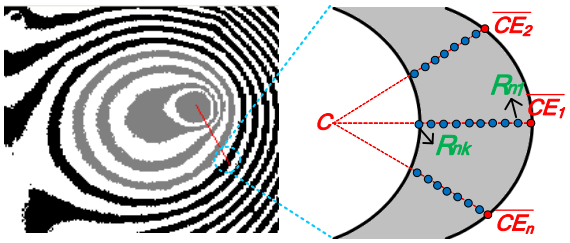

Fig. 6 Schematic diagram to determine the extremely dark point of radial lines

D. Using The Bezier Curve to Fit Micro-lens Profile Contour Lines

When the extremely bright point and the extremely dark point are determined, as there may be omitted points between these extreme points, neither the extremely bright fringe nor the extremely dark fringe are closed rings[9-11]. Therefore, the "Bezier curve" algorithm is modified in this study for curve fitting, where the fitted closed curve is the micro-lens profile contour line[12].

A second-order Bezier curve is used to fit the extremely bright fringes and the extremely dark fringes. The dark fringe is taken as an example, every three pixels of the extremely dark fringes is set as a group[13-14], and the extremely dark fringes are fitted with multi unit Bezier curves as shown in Figure 7.

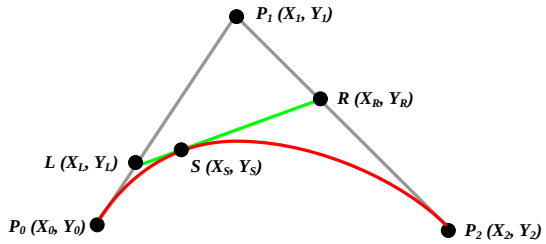

Fig. 7 A second-order Bezier curve is composed of P_0, S and P_2

The unit Bezier curve is composed of P_0, S and P_2, where P_0 is the start point of the unit Bezier curve, P_2 is the end point of the unit Bezier curve and P_1 is the control point of the unit Bezier curve. Point $S(t)$ varies from L to R forms a second-order Bezier curve, which can be expressed as follows:

$$S(t)=(1-t)^2 P_0+2t(1-t)P_1+t^2P_2,\ t\in[0,1]. \quad (3)$$

The complete micro-lens profile contour lines are shown in Figure 8, and the altitude difference soundness is the quadrant inspection light wavelength.

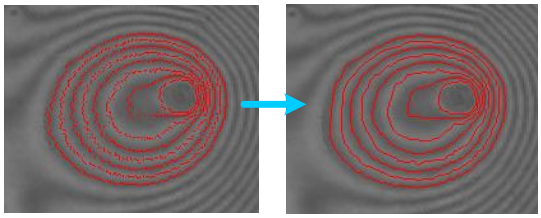

Fig. 8 Complete micro-lens profile contour lines

E. Rebuild Three-dimensional Pattern of Micro-lens

The phase angle of the interference fringes changes from 0° to 180°, indicating the microlens surface variation is λ/4. But the phase angle of the innermost ring is probably not a complete change. Finding maximum value T_i and minimum value D_i of the brightness curve of the i^{th} segment, $g(x,y)$ is brightness of pixel (x,y) on the i^{th} segment brightness curve.

Let Δ_i be the brightness variation of the i^{th} segment when the phase angle changes from 0° to 180°,

$$\Delta_i=|T_i-D_i|. \quad (4)$$

Let A_i be the brightness of the i^{th} segment at a phase angle of 90°,

$$A_i=D_i+\Delta_i/2. \quad (5)$$

The phase angle difference $\delta\,\theta(x,y)$ between the point (x, y) and $(x+1, y)$ in the i^{th} segment can be calculated as follows:

$$\delta\theta(x,y)=\cos^{-1}\left[2(g(x,y)-A_i)/\Delta_i\right]-\cos^{-1}\left[2(g(x+1,y)-A_i)/\Delta_i\right]. \quad (6)$$

where $g(x,y)$, $g(x+1, y)$ are the gray level of the point (x, y) and $(x+1, y.)$ The phase angle of the innermost interference fringe then can be calculated by the outer interpolation method.

Let the segment where center circle (x_c, y_c) lies be the n^{th} segment, then the corresponding microlens surface altitude difference $\delta d(x)$ between point (x, y) and $(x+1, y)$ in this segment can be obtained from the following equation [15-16]:

$$\delta\theta(x,y)=(\lambda/4\pi)\left|\cos^{-1}\left[2(g(x,y)-A_i)/\Delta_i\right]-\cos^{-1}\left[2(g(x+1,y)-A_i)/\Delta_i\right]\right|. \quad (7)$$

Summation of the corresponding microlens surface altitude difference from the 1^{st} segment to the $(n-1)^{th}$ segment and the n^{th} segment where the microlens center circle (x_c, y_c) lies, we can obtain lens sag (Δd):

$$\Delta d=(n-1)(\lambda/4)+\sum_{i}^{x_c}\delta d(x). \quad (8)$$

where i is the x coordinate of every pixel on the innermost contour line.

III. EXPERIMENTAL RESULTS AND DISCUSSION

Figure 9 shows the proposed system for the three-dimensional pattern of a micro-lens. The laser spot was eliminated by a rotary diffusing plate, the fiber optic light pipe transmits the light source into the microscope array, the 20x object lens, 2x Adapter, Navitar Manual Zoom Lens, and CCD camera form an imaging device, under which there was an XY-Table mobile carrier for precision positioning. The micro-lens sample was placed on the XY-Table mobile platform, and an optical flat was placed on the micro-lens sample as the reference plane for the interferometer. The above-mentioned equipment was mounted on a vibration-proof platform to form an AOI equipment for the micro-lens.

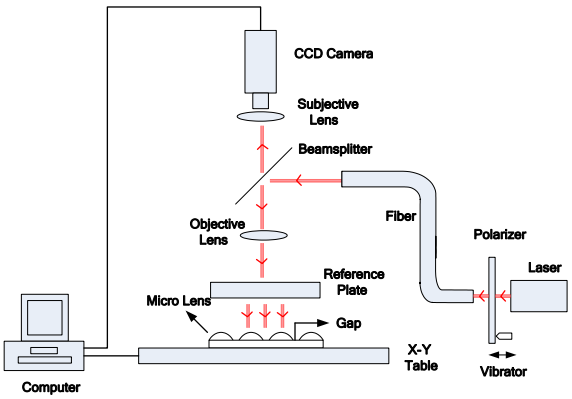

Fig. 9 Schematic diagram of inspection system structure

The unsymmetrical micro-lens was measured, as shown in Figure 10, and ten micro-lenses were randomly selected for measurement by this system. The lens sag measurement result was 1.39~1.45μm, ET-3000 surface profiler measurement result was 1.42μm, and the difference between them is less than 0.04μm. The three-dimensional pattern was rebuilt according to the aforesaid principle. Figure 11 is the curve diagram of micro-lens along the x axis according to

figure 8, and figure 12 is the top view of the rebuilt three-dimensional pattern of micro-lens.

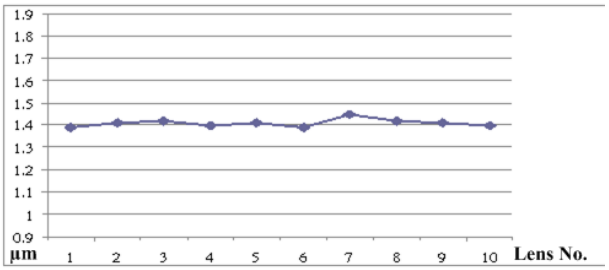

Fig. 10 The measurement result of lens sag of unsymmetrical micro-lenses obtained by this system

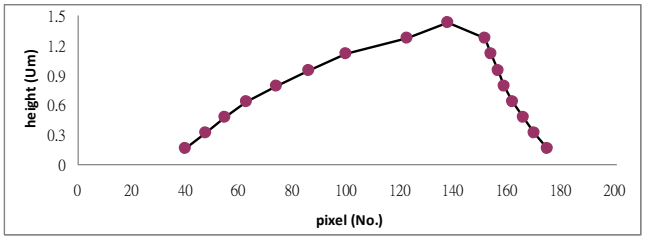

Fig. 11 The curve diagram of micro-lens along the x axis

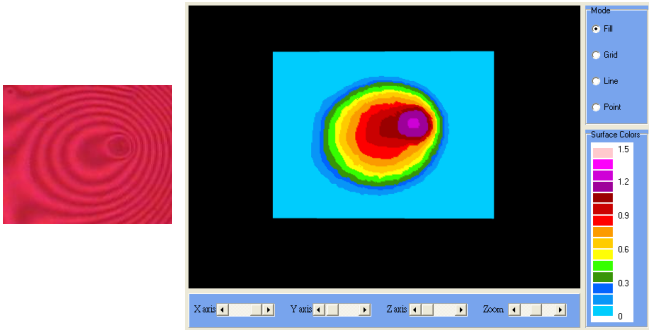

Fig. 12 Top view of three-dimensional pattern of unsymmetrical micro-lens

IV. CONCLUSIONS

The optical microscopic interferometric automatic inspection system for the three-dimensional pattern of a micro-lens array consists of an XY-Table, an optical imaging module, an optical interference module, and software controls. The XY-Table controls the longitudinal and transverse translation of the entire inspection system, and is able to individually inspect the lenses. The CCD camera captures the interference image of the micro-lens, the noise is first removed from the image, and then, the central position is searched using the region filling centroid method. Afterwards, the three-dimensional pattern of micro-lens is rebuilt using the contour line surface profile method, and the edge point coordinates of the annular interference fringes are individually determined through image processing and computer graphics. Each edge point of the dark and bright fringes can be connected to the center to form radial lines, and the coordinates of the interference fringe's extreme points on the radial lines can be determined. Since these extremely bright points and extremely dark points are not always a closed curve, the Bezier curve algorithm is introduced for curve fitting these points, which is the key innovation of this paper. Finally, the 3D surface profile of a micro-lens can be successfully rebuilt using the phase difference between the fringes.

As this system has the advantage of non-contact measurement, which does not require a metal coating to form a reflective surface for measurement, thus, avoiding the destruction of the surface structure of samples. Furthermore, the three-dimensional pattern of the micro-lens to be measured can be rebuilt, and as only one image is taken each time, the inspection process is rapid.

ACKNOWLEDGMENT

This work was sponsored by the Chung-Shan Institute of Science & Technology under Grant No. CSIST-757-V303 (100) and the National Science Council, under grant no. 99RA11.

REFERENCES

[1]. C. F. Tsou, C. W. Lin, New method for microlens fabrication by a heating encapsulated air process, Photonics Technology Letters, 18 (2006), 2490-2492

[2]. C. S Lin, C. W. Ho, S. W. Yang, , D.C. Chen, M. S.Yeh, Automatic optical inspection system for the image quality of microlens array. Indian Journal of Pure and Applied Physics. 48(9) (2010), 635-643

[3]. S. K. Rotich, J. G. Smith, A. G. R. Evans, A. Brunnschweiler, "Micromachined thin solar cells with a novel light trapping scheme", *Journal of Micromechanics and Microengineering*, 8(2) (1998), 134-137.

[4]. B. Ezell, "Making microlens backlights grow up", *Information Display*, 5 (2001), 21-26.

[5]. D. M. Hartmann, D. J. Reiley, S. C. Esener, "Microlenses self-aligned to optical fibers fabricated using the hydrophobic effect", *IEEE Photonics Technology Letters*, 13(10) (2001), 1088 – 1090.

[6]. D. L. MacFarlane, V. Narayan, J. A. Tatum, W. R. Cox, T. Chen, D. J. Hayes, "Microjet fabrication of microlens arrays", *IEEE Photonics Technology Letters*, 6(9) (1994), 1112-1114.

[7]. A. Yamamoto, I. Yamaguchi, "Surface profilometry by wavelength scanning Fizeau interferometer", *Optics and Laser Technology*, 32(4) (2000), 261-266.

[8]. F. Charriere, J. Kuhn, T. Colomb, F. Montfort, E. Cuche, Y. Emery, et al, "Characterization of microlenses by digital holographic microscopy", *Applied Optics*, 45(5) (2006), 829-835.

[9]. K. Hibion, B. F. Oreb, P. S. Fairman, J. Burke, Simultaneous measurement of surface shape and variation in optical thickness of a transparent parallel plate in wavelength-scanning Fizeau interferometer", Applied Optics, 43 (2004), 1241-1249.

[10]. C. S. Lin, C. H. Lin, D. C. Chen, C. L. Tien, M. S. Yeh, Measurement method of three-dimensional profiles of small lens with gratings projection and a flexible compensation system. Expert Systems with Applications. 38 (2011) 6232–6238

[11]. R. Bunnagel, H. A. Oehring, K. Steiner, Fizeau interferometer for measuring the flatness of optical surfaces, Applied Optics, 7 (1968) 331-335

[12]. C. S. Lin, S. C. Chang, Y. L. Lay, M. S. Yeh, C. J. Lee, Automatic distortion measuring system with reticle positioning for enhanced accuracy. Measurement. 41(9) (2008), 960-969.

[13]. C.S. Lin, , K.H. Huang, Y. L. Lay, , K. C. Wu, Y. C. Wu, J. M. Lin, An improved pattern match method with flexible mask for automatic inspection in the LCD manufacturing process. Expert Systems with Applications. 36 (2009). 3234–3239

[14]. M. Baba, K. Ohtani, A novel subpixel edge detection system for dimension measurement and object localization using an analogue-based approach. Pure and Applied Optics. 3 (2001), 276-283.

[15]. C. S. Lin, G. H. Loh, S. H. Fu, S. W. Yang, H. K. Chang & M. S. Yeh, "An automatic evaluation method for the surface profile of

the microlens array using an optical interferometric microscope", *Measurement Science and Technology*, 21(10) (2010), 1-10.

[16]. S. W. Yang, C. S. Lin, S. H. Fu, M. S. Yeh, C. Tsou, T. H. Lai, Lens sag measurement of microlens array using optical interferometric microscope, Optics Communications, 285(2012), 1066-1074.